Soleus responses to Achilles tendon stimuli are suppressed by heel and enhanced by metatarsal cutaneous stimuli during standing

Robyn L. Mildren[1], Ryan M. Peters[1,2], Mark G. Carpenter,[1,3,4] Jean-Sébastien Blouin,[1,3,5] and J. Timothy Inglis[1,3,4]

[1]*School of Kinesiology, University of British Columbia, Vancouver, British Columbia, Canada*
[2]*Faculty of Kinesiology, University of Calgary, Calgary, Alberta, Canada*
[3]*Djavad Mowafaghian Centre for Brain Health, University of British Columbia, Vancouver, British Columbia, Canada*
[4]*International Collaboration on Repair Discoveries, Vancouver, British Columbia, Canada*
[5]*Institute for Computing, Information and Cognitive Systems, University of British Columbia, Vancouver, British Columbia, Canada*

*Robyn L. Mildren: robyn.mildren@alumni.ubc.ca (corresponding author)
Ryan M. Peters: ryan.peters1@ucalgary.ca
Mark G Carpenter: mark.carpenter@ubc.ca
Jean-Sébastien Blouin: jean-sebastien.blouin@ubc.ca
J. Timothy Inglis: tim.inglis@ubc.ca

Running Title: Cutaneous modulation of the stretch reflex pathway during standing

Keywords: Cutaneous; Stretch reflex; Balance; Postural control; Muscle spindle

Key points

- We examined the influence of cutaneous feedback from the heel and metatarsal regions of the foot sole on the soleus stretch reflex pathway during standing.

- We found that heel electrical stimuli suppressed and metatarsal stimuli enhanced the soleus vibration response.

- Follow up experiments indicated that the interaction between foot sole cutaneous feedback and the soleus vibration response was likely not mediated by presynaptic inhibition and was contingent upon a modulation at the α-motoneuron pool level.

- The spatially organized interaction between cutaneous feedback from the foot sole and the soleus vibration response provides information about how somatosensory information is combined to appropriately respond to perturbations during standing.

Abstract

Cutaneous feedback from the foot sole provides balance relevant information and has the potential to interact with spinal reflex pathways. In this study, we examined how cutaneous feedback from the foot sole (heel and metatarsals) influenced the soleus response to proprioceptive stimuli during standing. We delivered noisy vibration (10-115 Hz) to the right Achilles tendon while we intermittently applied electrical pulse trains (five 1 ms pulses at 200 Hz, every 0.8-1.0 s) to the skin under the heel or metatarsals of the ipsilateral foot sole. We analyzed time-dependent (referenced to cutaneous stimuli) coherence and cross-correlations between the vibration acceleration and rectified soleus EMG. Vibration-EMG coherence was observed across a bandwidth of ~10-80 Hz, and coherence was suppressed by heel but enhanced by metatarsal cutaneous stimuli. Cross-correlations showed soleus EMG was correlated with the vibration (~40 ms lag) and cross-correlations were also suppressed by heel (from 104-155 ms) but enhanced by metatarsal (from 76-128 ms) stimuli. To examine the neural mechanisms mediating this reflex interaction, we conducted two experiments to probe potential contributions from 1) presynaptic inhibition, and 2) modulations at the α- and γ-motoneuron pools. Results suggest the cutaneous interactions with the stretch reflex pathway required a modulation at the α-motoneuron pool and were likely not mediated by presynaptic inhibition. These findings demonstrate that foot sole cutaneous information functionally tunes the stretch reflex pathway during the control of upright posture and balance.

Introduction

  Cutaneous afferents that innervate the foot sole can contribute to the control of standing balance. For example, reducing cutaneous feedback from the foot sole has been shown to impair balance (Meyer et al. 2004; Wang et al. 2016), while facilitating cutaneous feedback from the boundaries of the feet has been shown to improve stability (Maki et al. 1999). The postural (Kavounoudias 1998, 1999) and muscle responses that are evoked by cutaneous stimuli are spatially and temporally organized (Aniss et al., 1992; Nakajima et al., 2006). Specifically, stimuli applied under the heel facilitate ankle plantar flexor muscle activity and inhibit dorsiflexor muscle activity, whereas stimuli applied under the metatarsals evoke responses of opposite polarity (Aniss et al., 1992; Nakajima et al., 2006). Muscle responses evoked by cutaneous stimuli are also modulated in a task dependent manner. Cutaneous reflex gain is lower during standing relative to sitting (Aniss et al., 1992) and reflex polarity can reverse during different phases of the gait cycle (Zehr et al., 1997, 2012, 2014). Low threshold (tactile) cutaneous afferents have dispersed projections to the spinal cord; there is evidence they interact with Ia and Ib inhibitory interneurons (Lundberg et al., 1977; Bergego et al., 1981; Pierrot-Deseilligny et al., 1981; Rossi and Mazzocchio, 1988), primary afferent depolarization (PAD) interneurons (Iles, 1996), as well as γ-motoneurons

(Hunt et al., 1951; Alnaes et al., 1965; Appelberg et al., 1977; Aniss et al., 1988, 1990). While the net cutaneous reflex is spatially organized according to the skin region stimulated (Aniss et al., 1992; Nakajima et al., 2006), less is known about the spatial organization of cutaneous interactions with other spinal reflex pathways during standing.

  The interactions between two different sensory inputs to the spinal cord can be assessed using a condition-test paradigm, where a conditioning stimulus (e.g., cutaneous electrical pulses) is delivered at a pre-defined interval relative to a test stimulus (e.g., mixed nerve stimulation to evoke the H-reflex). Using this paradigm, electrical stimulation of the skin under the metatarsals has been shown to inhibit the soleus H-reflex at short condition-test intervals (6-60 ms, Knikou et al., 2007; 25-40 ms, Sayenko et al., 2009; 45 ms, Lowrey and Bent, 2009) while stimulation of the skin under the heel has been shown to facilitate the soleus H-reflex at a 50 ms condition-test interval (Sayenko et al. 2009). Although presynaptic

inhibition via PAD interneurons has been speculated as a potential mechanism of cutaneous-H-reflex interaction, confirming the presence of other properties of presynaptic inhibition would further support this theory. Specifically, reflex amplitude modulations induced by presynaptic inhibition should be dissociated from modulations in α-motoneuron pool excitability, occur early and have a prolonged duration, and preferentially affect low frequency responses (Eccles et al., 1962; Morita et al., 1998, 2001; Rudomin and Schmidt, 1999; Pierrot-Deseilligny and Burke, 2012). The condition-test stimulus approach, however, does not provide information about the response frequency characteristics and the pre-defined condition-test intervals provide poor temporal resolution. In addition, mixed nerve stimuli (e.g. H-reflex) and tendon taps perturb standing balance (Mynark and Koceja, 2002; Mildren et al. 2017), which limits their usefulness for understanding reflex interactions specific to upright posture and balance control.

To overcome some limitations associated with the condition-test stimulus approach, here we delivered continuous proprioceptive stimuli (noisy Achilles tendon vibration; Mildren et al. 2017, 2019) along with intermittent cutaneous stimuli (electrical pulse trains) to reveal modulations in time-dependent vibration-EMG coherence and cross-correlations evoked by cutaneous input. The primary aim of this study was to characterize the interaction between cutaneous inputs from the heel and metatarsals of the foot sole and the soleus response to Achilles tendon vibration during standing. We hypothesized that heel and metatarsal cutaneous stimuli would evoke opposite changes in the soleus response to vibration (enhancement vs. suppression). Next, we explored the potential roles of presynaptic inhibition and modulations at the α- and γ-motoneuron pools in mediating cutaneous interactions with the soleus vibration response. To characterize the influence of presynaptic inhibition on vibration-EMG coherence and cross-correlations, we stimulated the deep branch of the common fibular (CF) nerve, since group I afferents in the CF nerve are known to activate PAD interneurons that mediate presynaptic inhibition (Eccles et al., 1962; Hultborn et al., 1987; Rudomin and Schmidt, 1999). We expected that if presynaptic inhibition plays a role in gating trains of afferent input generated by noisy vibration, then CF nerve stimuli would evoke an early and prolonged suppression of vibration-EMG coherence

preferentially in the low frequency bandwidth. To examine the potential contribution from γ-motoneurons, we reduced the current of the electrical stimulus to the skin since γ-motoneurons have been shown to have a lower threshold to cutaneous input relative to α-motoneurons (Hunt, 1951; Eldred and Hagbarth, 1954; Alnaes et al., 1965; Appelberg et al., 1977). We expected that if stimuli targeting γ-motoneurons induced a modulation in coherence and cross-correlations, then this would support involvement of γ-motoneurons as a mechanism mediating cutaneous interaction with the stretch reflex pathway.

Methods

Ethical approval

Written informed consent was obtained and the University of British Columbia Research Ethics Board approved all procedures (H12-01698). This study conformed to the standards set by the Declaration of Helsinki, except for registration in a database.

Participants

A total of 24 healthy young adults (age = 24.0 ± 3.0 yrs; 15 males, 9 females), free of musculoskeletal and neurological disorders, participated in this study.

Experimental setup

Participants stood on a force plate (OR6-7; AMTI, USA; forces and moments amplified ×1000-4000 and sampled at 100 Hz) with their stance width equal to their foot length. Participants first completed a 2-min quiet standing trial and ± 2 standard deviation (SD) bandwidths were calculated around mean centre of pressure (COP) position in the anteroposterior and mediolateral directions. We monitored COP position in subsequent trials and provided verbal feedback if COP drifted outside of this bandwidth. Noisy vibration was continuously applied to the right Achilles tendon for 2 mins while electrical stimuli were delivered intermittently (every 0.8-1.0 s) to the heel or metatarsals (*see Experiment 1: Heel and metatarsal stimuli*), the CF nerve (*see Experiment 2: Involvement of presynaptic inhibition*), or the metatarsals at a lower current amplitude (*see Experiment 3: Involvement of α- and γ-motoneuron pools*).

Surface electromyography (EMG) was recorded in a bipolar configuration unilaterally from the right soleus and tibialis anterior muscles through surface electrodes placed over the muscle bellies with the ground placed on either the medial or lateral malleolus. We chose to examine responses in the soleus muscle since it has previously been shown to exhibit stronger vibration responses relative to the gastrocnemii in both surface EMG (Mildren et al. 2017) and indwelling EMG (Mildren et al. 2019). EMG data were amplified ×2000, bandpass filtered 10-1000 Hz (NeuroLog NL824 preamplifier and NL820 Isolator; Digitimer, UK), and sampled at 2000 Hz (Power 1401 A/D board and Spike2 software; Cambridge Electronic Design, UK).

Mechanical stimuli were applied to the right Achilles tendon through a 3 cm diameter probe controlled by a linear motor (model MG-160; Labworks, USA). The probe of the linear motor was pulled into the tendon using a weighted pulley system to maintain a preload force of ~1 N. The pre-load force and acceleration of the probe on the Achilles tendon were sensed using a force transducer (model 31; Honeywell, USA) and a linear accelerometer (model 220-010; X Tronics, CA), respectively. Force and acceleration signals were differentially amplified (force ×100, acceleration ×1), low-pass analogue filtered at 600 Hz (Brownlee model 440; NeuroPhase LLC, USA), and sampled at 2000 Hz (Power 1401 A/D board and Spike2 software; Cambridge Electronic Design, UK). A white noise signal was generated and low-pass filtered at 100 Hz using LabVIEW 11 software and sent to a motor amplifier (PA-141; Labworks, USA) to control noisy tendon vibration. In the recorded probe acceleration data, power at frequencies beyond a bandwidth 10-115 Hz was $\leq$ -13 dB (ref. peak plateau of power spectrum) (Mildren et al., 2017), and the root-mean-square amplitude of the vibration acceleration was 15 m/s^2.

Experiment 1: Heel and metatarsal stimuli

Twelve adults (7 males, 5 females) participated in Experiment 1. To investigate the influence of foot sole cutaneous feedback on the soleus response to tendon vibration, we applied electrical stimuli to the heel or metatarsal regions of the right foot sole along with tendon vibration. Six 2-min trials were conducted for each condition (heel and metatarsal stimuli) in block randomized order. Cutaneous stimuli were applied through 5 cm diameter

adhesive electrodes (Dermatrode type 00200-340; Delsys, USA) (Fig. 1). For heel stimuli the anode was placed under the proximal aspect and the cathode under the distal aspect of the heel, and for metatarsal stimuli the anode was placed under the first metatarsal and the cathode under the fourth and fifth metatarsals. Using a constant current stimulator (DS7A Constant Current Stimulator, Digitimer, UK) controlled through Spike2 software, trains of five 1 ms square-wave pulses at 200 Hz were delivered with a 0.8-1.0 s inter-stimulus-intervals (ISI). This variability in ISI was programmed to minimize predictability of the cutaneous stimuli. Perceptual threshold was found by increasing the stimulus intensity until participants detected the pulse trains under the foot, and then decreasing the intensity until they no longer perceived the pulses. Several reversals of stimulus intensity were performed until a consistent threshold was found. All subsequent stimuli were delivered at $2\times$ perceptual threshold.

Experiment 2: Involvement of presynaptic inhibition

Six adults participated in Experiment 2 (4 males, 2 females), one had also participated in Experiment 1. Experiment 2 was conducted to examine whether presynaptic inhibition has the capacity to gate vibration responses, and therefore the potential to mediate cutaneous interactions with the stretch reflex pathway. Group I (Ia and Ib) afferents in the CF nerve that innervate receptors in ankle dorsiflexor muscles are known to provide strong input to PAD interneurons that regulate transmission through primary afferent terminals of ankle plantar flexor muscles (Eccles et al., 1962; Hultborn et al., 1987; Rudomin and Schmidt, 1999). Therefore, we electrically stimulated the deep branch of the CF nerve to provide excitatory input to PAD interneurons that mediate presynaptic inhibition while we applied noisy Achilles tendon vibration. It was expected that if presynaptic inhibition can play a role in controlling the vibration response, then it would manifest as an early and long-lasting inhibition of vibration-EMG coherence and cross-correlations following CF nerve stimuli. A 4.5×9.5 cm diameter carbon rubber electrode coated with conductive gel (Spectra 360, Parker Laboratories, USA) was placed just above the patella as the reference, and a custom metal ballpoint electrode was used to search for the deep branch of the CF nerve around the fibular head. Specifically, we searched for the stimulus location that produced activity in

muscles innervated by the deep branch of the CF nerve (e.g., tibialis anterior, toe extensors, fibularis tertius) along with paresthesia between the hallux and second digit, in the absence of activity in muscles innervated by the superficial branch of the CF nerve (e.g., fibularis longus and brevis). The custom electrode was then replaced with an adhesive 1 × 1 cm diameter EMG electrode (Kendall cloth electrode) and the current threshold needed to evoke a just noticeable M-wave (present in ~2/3 stimuli) in tibialis anterior from individual stimuli was identified by viewing stimulus-triggered surface EMG in Spike2 software. The CF nerve stimulus intensity was maintained at 1.3 × M-wave threshold for tibialis anterior (Pierrot-Deseilligny and Burke, 2012); M-wave threshold was re-assessed if the M-wave amplitude changed during a trial or if the participant took a seated break between trials. We applied single electrical pulses to the deep branch of the CF nerve intermittently (every 0.8-1.0 s) while we applied noisy Achilles tendon vibration over six 2-min standing trials.

Experiment 3: Involvement of α- and γ-motoneuron pools

Ten adults participated in Experiment 3 (6 males, 4 females); two had participated in Experiment 1, and one had participated in both Experiments 1 and 2. This experiment was conducted to examine the roles of the α- and γ-motoneuron pools in the interaction between cutaneous feedback and the vibration response. There is evidence that γ-motoneurons have a lower threshold to cutaneous input relative to α-motoneurons (Hunt, 1951; Eldred and Hagbarth, 1954; Alnaes et al., 1965; Appelberg et al., 1977). Therefore, a modulation in vibration-EMG coherence and cross-correlations in the absence of a cutaneous reflex would support involvement of cutaneous projections to γ-motoneurons. Conversely, the presence of a modulation in vibration-EMG coherence and cross-correlations only when a cutaneous reflex is evoked would suggest that a change in the excitability of the α-motoneuron pool is necessary to observe a cutaneous interaction with the stretch reflex pathway. We identified the highest cutaneous stimulation intensity that could be applied to the metatarsals without evoking a cutaneous reflex in soleus rectified trigger-averaged surface EMG based on a minimum of 50 stimulus pulse trains (5 pulses at 200 Hz, 0.4-0.6 s ISI). This stimulation intensity was typically just above perceptual threshold. We then applied this stimulus level to

the metatarsals (5 pulses at 200 Hz, every 0.8-1.0 s) along with noisy tendon vibration over six 2-min standing trials.

Data analyses and statistics

To examine changes in proprioceptive responses following cutaneous stimuli, we calculated time-dependent coherence and cross-correlations. Coherence describes the linear correlation between the vibration and muscle activity across frequencies, and significant vibration-EMG coherence is typically found in soleus across a bandwidth of ~10-80 Hz (Mildren et al. 2017; 2019). Here, time-dependent coherence was used to examine how coherence varies following the stimuli. Cross-correlations describe the correlation between the vibration and muscle activity as the EMG is lagged in time relative to the stimulus. Cross-correlations typically demonstrate that the EMG is correlated with the stimulus at a ~40 ms lag time, which corresponds to the latency of tendon tap responses (Mildren et al. 2017, 2019). Here, time-dependent cross-correlations were used to examine how correlation amplitudes change following cutaneous stimuli. First, EMG and acceleration data were digitally low-pass filtered at 600 Hz (4th order dual pass Butterworth filter) and EMG data were full-wave rectified. Stimulus artifacts in the EMG from the electrical pulses were replaced with mean EMG (therefore, the stimulus artifact location will appear in figures as a band of coherence and correlation strength equal to zero). For the time-dependent coherence and cross-correlation analyses, epochs of data were extracted from 250 ms before to 750 ms after the onset of each stimulus train; this provided ~770 epochs of data for each participant over the six 2-min trials of each condition (heel and metatarsal stimuli in Experiment 1, CF nerve stimuli in Experiment 2, and below threshold metatarsal stimuli in Experiment 3). We were primarily interested in the ~500 ms window following the cutaneous stimuli; therefore, the analyzed epochs provided ~250 ms of padding on either side of the window of interest (e.g., a full cycle of vibration at 5 Hz on either side, where our bandwidth of interest was ~10-80 Hz; Mildren et al. 2017). The last stimulus at the end of a trial was removed if there was an incomplete (<750 ms) epoch of data following it.

Due to the nonstationarity of the EMG data, a Morlet wavelet decomposition method (Zhan et al., 2006; Blouin et al., 2011) was used to calculate time-dependent coherence

(referenced to the onset of the cutaneous stimuli). This analysis was performed for data pooled across participants for each condition. Coherence [$C(t,f)$] was estimated using the following equation:

$$C(t, f) = \frac{|P_{xy}(t, f)|^2}{P_{xx}(t, f) P_{yy}(t, f)}$$

Where t is time with respect to the cutaneous pulse train, f is frequency, $P_{xy}(t,f)$ is the cross-spectrum of the probe acceleration and EMG signals, and $P_{xx}(t,f)$ and $P_{yy}(t,f)$ are the auto-spectra of the acceleration and EMG signals, respectively. Time-dependent coherence values were considered significant when they exceeded 99% confidence limits, since a 99% limit was shown to better represent an α-level of 0.05 due to the bidirectional nature of the data (Blouin et al., 2011). All non-significant coherence values were set to 0. For Experiment 3, time-dependent coherence [$C(t,f)$] and time-dependent EMG power spectra [$P_{yy}(t,f)$] were also examined on an individual participant bases to identify if any changes in coherence were associated with changes in EMG power. Time-dependent cross-correlations with respect to the electrical pulse trains were calculated using a custom-written algorithm in Matlab (Blouin et al. 2011; available from http://persianney.com/kvdoelcsubc/pubs.html) using the convention a positive correlation reflects that acceleration into the tendon is associated with an increase in rectified EMG. Time-dependent cross-correlations were examined on an individual participant bases to extract information about the latency and duration of the modulation in the vibration response following cutaneous stimuli.

First, we quantified baseline coherence and cross-correlations over time without the influence of stimuli by randomly generating trigger times with an ISI of 0.8-1.0 s and used these as references for the time-dependent coherence and cross-correlation analyses. We examined the change in peak-to-peak (P2P) amplitude of the cross-correlations following electrical pulses (or randomly generated trigger times). Specifically, on an individual participant basis, we extracted the P2P amplitude of the cross-correlations over time following the stimuli; i.e., the maximum minus the minimum correlation amplitude was extracted along the correlation lag time axis, and then examined along the time axis following stimuli (see example for one participant in Fig. 3B and C). To examine how the

vibration-evoked muscle response was influenced by the stimuli, the change in P2P amplitude over time following cutaneous stimuli (P2P amplitude minus the mean) was then averaged across participants. The change in P2P cross-correlation amplitude over time following randomly generated trigger times was also extracted and used to calculate the SD over a 400 ms window following the trigger times for both the heel and metatarsal conditions. This SD was used to construct ± 2 SD bandwidths around the P2P cross-correlation, and the onset of a significant phasic modulation was identified as the latency when P2P cross-correlation values crossed a positive or negative 2-SD threshold and remained outside of this threshold for a minimum of 20 consecutive data points (10 ms). Similarly, the offset of the modulation was identified as the time when the P2P cross-correlations returned and remained within the ± 2 SD bandwidth for a minimum of 20 consecutive data points.

To determine whether there was a tonic modulation of the vibration-evoked response induced by heel and metatarsal stimuli, the mean P2P cross-correlation amplitude over the entire length of the trials was compared between heel and metatarsal conditions using a paired samples *t*-test. To examine whether there were differences between the modulation latencies from heel vs. metatarsal stimuli, for each participant, the latency of the maximum change in P2P cross-correlation strength following heel and metatarsal stimuli was extracted and compared between heel and metatarsal conditions using a paired samples *t*-test.

To examine the change in soleus EMG evoked by heel, metatarsal, and CF nerve stimuli, EMG data were trigger-averaged to the onset of the electrical pulses. The resulting waveform average for each participant was then debiased and averaged across participants. To align the stimulus artifact in the EMG with the artifact in the cross-correlation, the EMG was shifted in time by 42 ms in the negative direction to correspond to the lag time where the vibration and EMG were correlated (since the EMG was correlated with stimulus acceleration when shifted ~42 ms backward in time due to the neural transmission delay).

Results

Experiment 1: Heel and metatarsal stimuli

Data referenced to randomly generated trigger times revealed that vibration-EMG coherence was significant (above 99% confidence limits) across a bandwidth of ~10-80 Hz, with the strongest coherence around 40 Hz and minimal variation over time (Fig. 2; top panel). Soleus EMG was correlated with the vibration when lagged by ~40 ms relative to the vibration acceleration signal (Fig. 2; bottom panel), with minimal variation in P2P amplitude over time when referenced to the randomly generated trigger times. The SD in P2P amplitude over time was 0.0104 during the heel condition, and 0.0114 during the metatarsal condition; therefore, the ± 2 SD bandwidths used to analyze modulations in P2P amplitude were ± 0.0208 and ± 0.0228, respectively.

Data referenced to the cutaneous stimuli revealed that coherence was suppressed by heel stimuli and enhanced by metatarsal stimuli at latencies of ~100 ms (representative data are presented in Fig. 3A, and group data are presented in Fig. 4A). The peak of the cross-correlation occurred at a lag time of 39.6 ± 3.1 ms during heel stimuli, and 39.1 ± 3.0 ms during metatarsal stimuli. The average P2P cross-correlation amplitude was not significantly different between heel (r = 0.27 ± 0.08) and metatarsal (r = 0.29 ± 0.07) conditions [$t_{(11)}$ = -1.360, p = 0.201], which suggests there was minimal tonic effect of the electrical pulse trains on vibration responses. Cross-correlation strength was similarly suppressed and enhanced by heel and metatarsal stimuli, respectively, at ~100 ms latencies (representative cross-correlation data are presented in Fig. 3B). To further assess the time course of this suppression and enhancement, the P2P cross-correlation was examined over time following the cutaneous stimuli (Fig. 3C). The change in P2P cross-correlation amplitude over time averaged across participants demonstrated that cross-correlations were suppressed (exceeding the 2 SD negative limit) at 104 ms and returned to baseline at 155 ms following heel stimuli (Fig. 4B). Following metatarsal stimuli, the cross-correlations were enhanced (exceeding the 2 SD positive limit) at 76 ms and returned to baseline at 128 ms (Fig. 4B). The maximum modulation in cross-correlation strength occurred significantly earlier for metatarsal stimuli (peak increase at 96 ± 14 ms) compared to heel stimuli (peak decrease at 118 ± 23 ms) [$t_{(11)}$ =

2.849, p = 0.016). After subtraction of the cross-correlation lag time, heel cutaneous stimuli evoked an increased followed by a decrease in rectified surface EMG (peak decrease at 104 ± 8 ms latency), while metatarsal stimuli evoked a decrease followed by an increase (peak increase at 86 ± 10 ms latency) (Fig. 4B). Thus, the modulations in vibration responses due to cutaneous input were not clearly dissociated from the changes in background EMG.

Experiment 2: Role of presynaptic inhibition

In soleus surface EMG, CF nerve stimuli evoked an early and short-lasting inhibition that resembled the characteristics of disynaptic reciprocal inhibition (based on polarity, latency, and duration), followed by a prolonged increase in EMG lasting ~100 ms (Fig. 5B). In vibration-EMG coherence, we observed no evidence of an inhibition; instead, CF nerve stimuli evoked an early and prolonged facilitation in coherence (Fig. 5A). The change in P2P cross-correlation strength following CF nerve stimuli similarly demonstrated an early and prolonged facilitation (Fig. 5B).

Experiment 3: Involvement of α- and γ-motoneuron pools

To examine whether the modulation from foot sole stimuli could be evoked at stimulus levels that preferential target γ-motoneurons, we reduced the metatarsal stimulus current to below the threshold to evoke a cutaneous reflex in soleus surface EMG during standing. Despite the absence of a cutaneous reflex (averaged over a minimum of 50 stimuli) during quiet standing, when we added tendon vibration, a cutaneous reflex emerged in four out of 10 participants. Fig. 6A demonstrates trigger-averaged soleus EMG for a participant that showed evidence of a cutaneous reflex at a latency of ~100 ms when tendon vibration was added. Similarly, Fig. 6B demonstrates the emergence of a cutaneous reflex in time-dependent EMG power across a bandwidth of ~20-60 Hz at a ~100 ms latency following cutaneous stimuli. In contrast, Fig. 6C shows a participant that did not demonstrate a cutaneous reflex when tendon vibration was added to subthreshold cutaneous electrical stimuli. Across participants, there was no evidence that a modulation in vibration-EMG coherence was evoked in the near absence of a cutaneous reflex. Overall, these data indicate a modulation in vibration-EMG coherence via cutaneous input necessitates a change in α-

motoneuron pool excitability.

Discussion

To examine how foot sole cutaneous feedback interacts with the soleus stretch reflex pathway during standing, we examined the change in coupling between tendon stimuli and soleus EMG over time following foot sole electrical stimuli (heel vs. metatarsals). Our results showed that cutaneous stimuli applied to the heel suppressed the vibration response in soleus, demonstrated by a suppression of vibration-EMG coherence and cross-correlations. Conversely, cutaneous stimuli applied to the metatarsal enhanced the soleus response (enhancement of vibration-EMG coherence and cross-correlations) at a shorter latency relative to the effects of heel stimuli. We further explored potential mechanisms that mediate the observed interaction between cutaneous input and the soleus vibration response (Experiments 2 and 3). Results from those experiments suggest that the interaction was only present when the cutaneous stimuli induced a modulation in α-motoneuron excitability and the interaction was likely not mediated by presynaptic inhibition or selective input to γ-motoneurons.

Our finding of relatively late (~100 ms) modulations in the soleus vibration response contrasts with previous studies that observed earlier modulations (~40 ms latencies) in soleus H-reflex amplitude evoked by foot sole conditioning stimuli (Sayenko et al., 2007, 2009; Knikou, 2007, 2010; Lowrey and Bent, 2009). In addition to occurring earlier, the cutaneous modulation of the H-reflex was also in the opposite direction (heel facilitatory, metatarsals inhibitory) relative to the modulations in correlation strength observed in our experiment (heel suppression, metatarsals enhancement). The difference between our findings and those of previous studies (Sayenko et al., 2007, 2009; Knikou, 2007, 2010; Lowrey and Bent, 2009) could be attributed to differences in the posture of the participants (standing vs. seated or prone) or the methodological approach. Specifically, since cutaneous reflexes are task dependent, their interaction with the stretch reflex pathway may vary according to the posture and whether the muscles are engaged in the control of balance. Methodologically, the H-reflex is very sensitive to α-motoneuron pool excitability and presynaptic inhibition, whereas

the stretch and tendon tap responses are less sensitive to presynaptic inhibition (Morita et al., 1998; Enríquez-Denton et al., 2002). The lower sensitivity of mechanically generated trains of spindle input to presynaptic inhibition may be one explanation for why we did not observe a suppression in coherence and cross-correlations in response to CF nerve stimuli (Experiment 2). Another difference between H-reflex vs. tendon vibration methodologies is that the response evoked by tendon vibration involves mechanotransduction, and is therefore sensitive to changes in spindle sensitivity via γ-motoneuron activity. However, our results from Experiment 3, where stimuli were delivered at a level to target γ-motoneurons, do not suggest that the cutaneous interaction was mediated by a change in γ-motoneuron activity.

Therefore, our findings suggest that cutaneous input influences the transmission through the stretch reflex pathway via a modulation at the α-motoneuron pool.

Enhancement of correlations following CF nerve stimuli

We hypothesized that if input to PAD interneurons was capable of evoking presynaptic inhibition of the vibration response, this could be a potential mechanism for the cutaneous interactions. We did not observe any evidence that input to PAD interneurons from group I afferents in the CF nerve could evoke an inhibition of the vibration responses. Instead, we observed an early and prolonged enhancement in vibration-EMG coherence and cross-correlations. While an enhancement could be evoked by the stimulation of antagonist Ib afferents in the CF nerve, the duration of this facilitation was longer than would be expected from Ib input (Pierrot-Deseilligny and Burke, 2012); therefore, other mechanism such as presynaptic facilitation may also contribute to this enhancement.

Since the early description of presynaptic inhibition by Frank and Fuortes (1957), and pioneering work by Eccles and colleagues (1962), there have been recent findings that suggest PAD may have more complex functions in the regulation of afferent transmission (Li et al., 2017; Lucas-Osma et al., 2018). Activation of GABA receptors generates afferent depolarization, which causes presynaptic inhibition through action potential shunting at afferent terminals (Cattaert and Manira, 1999; Willis, 2006). However, it has been proposed that afferent depolarization by GABA receptors at branch points could facilitate transmission

by preventing conduction block (Li et al., 2017; Lucas-Osma et al., 2018), which may be a common occurrence in long and highly branched nerve fibres (such as muscle spindle afferents). The change in time-dependent coherence and cross-correlations we observed following CF nerve stimuli could reflect facilitation of afferent transmission; however, more experiments are necessary to confirm this possibility.

Role of α- and γ-motoneuron pools

We did not observe a modulation in vibration-EMG coherence in the absence of a cutaneous reflex. Our approach targeted the potential role of γ-motoneurons in the cutaneous modulation of the soleus responses since they exhibit a lower threshold to cutaneous input relative to α-motoneurons (Hunt, 1951; Eldred and Hagbarth, 1954; Alnaes et al., 1965; Appelberg et al., 1977). Our results do not support selective involvement of γ-motoneurons in mediating the cutaneous interaction with the stretch reflex pathway. Although cutaneous influences on γ-motoneuron activity have been demonstrated in animal experiments (Hunt, 1951; Eldred and Hagbarth, 1954; Alnaes et al., 1965; Appelberg et al., 1977), evidence from human studies is limited. Aniss et al. (1990) found indirect evidence of cutaneous modulation of γ-motoneuron activity (modulation of spindle afferent firing not explained by muscle stretch) in a small sample of ankle dorsiflexor spindle afferents in standing participants. Gandevia et al. (1994) also found indirect evidence of cutaneous modulation of γ-motoneuron activity in a small sample of spindle afferents recorded from forearm extensor muscles.

In some participants (n = 4), the previously subthreshold metatarsal cutaneous stimuli became suprathreshold when we added noisy tendon vibration, i.e. the cutaneous stimuli evoked a response in soleus EMG. This indicates that the vibration-evoked proprioceptive input to the spinal cord might facilitate the pathway involved in generating the cutaneous reflex. In individuals with a spinal cord injury, it has been shown that tendon vibration suppresses the late spasm-like cutaneous reflex activity in the antagonist muscle, possibly through inhibition of persistent inward currents via Ia inhibitory interneurons (DeForest et

al., 2020). Properly targeted tendon vibration could therefore present a method to either help facilitate activity in paretic muscles, or conversely control unwanted spasm like activity in antagonist muscles.

Functional implications

During standing, it is important that available information is integrated into the stretch reflex pathway so responses are adapted to the current situation. Our results support a potential functional contribution of cutaneous input to spinal cord circuitry for the control of movement and balance as proposed by van Wezel et al. (1997, 2000) and Zehr et al. (1997, 2012, 2014). In a backward leaning posture, it would be advantageous for cutaneous feedback from the heels to suppress the soleus stretch response that would increase the risk of falling backward. Conversely, metatarsal cutaneous feedback during a forward lean would help support the reflex activation of soleus and the generation of plantar flexion torque toward a neutral posture. Similarly, a forward perturbation (such as a push) during standing would cause an anterior shift in pressure under the feet as well as stretch of the triceps surae muscles. In this situation, cutaneous and proprioceptive information may be combined to enhance the plantar flexor muscle response to help prevent a forward fall. Overall, our results suggest that different regions of the foot sole have a functional role in tuning proprioceptive responses for the control of standing posture and balance.

Conclusions

In summary, our findings demonstrate spatially organized spinal interactions between foot sole cutaneous and triceps surae proprioceptive feedback in humans during standing. Specifically, heel stimuli suppressed while metatarsal stimuli enhanced the soleus muscle response to noisy Achilles tendon vibration. Results from our experiments also suggest this interaction required a strong enough cutaneous stimulus to modulate the α-motoneuron pool and was likely not mediated by presynaptic inhibition or γ-motoneurons. These findings indicate that cutaneous feedback from the foot sole is integrated into the stretch reflex pathway to functionally modulate (suppress or enhance) responses to proprioceptive stimuli during standing.

Data availability statement

The data that support the findings of this study are available on request from the corresponding author. The data are not publicly available due to privacy or ethical restrictions.

Competing interests

No conflicts of interest are declared by the authors.

Author contributions

R.L.M. was responsible for conception and design of the study, data acquisition, analysis, interpretation of data, and drafting and revising the manuscript. R.M.P., M.G.C., and J-S.B. were involved in interpretation of data and revising the manuscript. J.T.I. was involved in conception and design of the study, interpretation of data, and revising the manuscript. All authors approved the final version of the manuscript, agree to be accountable for all aspects of the work in ensuring that questions related to the accuracy or integrity of any part of the work are appropriately investigated and resolved, and all persons designated as authors qualify for authorship, and all those who qualify for authorship are listed.

References

Alnaes E, Jansen JK, & Rudjord T (1965). Fusimotor Activity in the Spinal Cat. *Acta Physiol Scand* 63, 197–212.

Aniss AM, Diener HC, Hore J, Gandevia SC, & Burke D (1990). Behavior of human muscle receptors when reliant on proprioceptive feedback during standing. *J Neurophysiol* 64,

661–670.

Aniss AM, Gandevia SC, & Burke D (1992). Reflex responses in active muscles elicited by stimulation of low-threshold afferents from the human foot. *J Neurophysiol* 67, 1375–1384.

Aniss AM, Gandevia SC, & Burke D (1988) Reflex changes in muscle spindle discharge during a voluntary contraction. *J Neurophysiol* 59, 908–921.

Appelberg B, Johansson H, & Kalistratov G (1977). The influence of group II muscle afferents and low threshold skin afferents on dynamic fusimotor neurones to the triceps surae of the cat. *Brain Res* 132, 153–158.

Bergego C, Pierrot-Deseilligny E, & Mazieres L (1981). Facilitation of transmission in Ib pathways by cutaneous afferents from the contralateral foot sole in man. *Neurosci Lett* 27, 297–301.

Blouin JS, Dakin CJ, van den Doel K, Chua R, McFadyen BJ, & Inglis JT (2011). Extracting phase-dependent human vestibular reflexes during locomotion using both time and frequency correlation approaches. *J Appl Physiol* 111, 1484–1490.

Cattaert D, & El Manira A (1999). Shunting versus inactivation: analysis of presynaptic inhibitory mechanisms in primary afferents of the crayfish. *J Neurosci* 19, 6079–6089.

DeForest BA, Bohorquez J, & Perez MA (2020). Vibration attenuates spasm-like activity in humans with spinal cord injury. *J Physiol* 13, 2703–2717.

Eccles JC, Schmidt RF, & Willis WD (1962). Presynaptic inhibition of the spinal monosynaptic reflex pathway. *J Physiol* 161, 282–297.

Eldred E, & Hagbarth KE (1954). Facilitation and inhibition of gamma efferents by stimulation of certain skin areas. *J Neurophysiol* 17, 59–65.

Enríquez-Denton M, Morita H, Christensen LO, Petersen N, Sinkjaer T, Nielsen JB (2002). Interaction between peripheral afferent activity and presynaptic inhibition of Ia afferents in the cat. *J Neurophysiol* 88, 1664–1674.

Frank K, & Fuortes MGF (1957). Presynaptic and postsynaptic inhibition of monosynaptic reflexes. *Fed. Proc* 16, 39–40.

Gandevia SC, Wilson L, Cordo PJ, & Burke D (1994). Fusimotor reflexes in relaxed forearm muscles produced by cutaneous afferents from the human hand. *J Physiol* 479(Pt 3), 499–508.

Hultborn H, Meunier S, Morin C, & Pierrot-Deseilligny E (1987). Assessing changes in

presynaptic inhibition of I a fibres: a study in man and the cat. *J Physiol* 389, 729–756.

Hunt, C.C. (1951). The reflex activity of mammalian small-nerve fibres. *J Physiol*. 115, 456–469.

Iles JF (1996). Evidence for cutaneous and corticospinal modulation of presynaptic inhibition of Ia afferents from the human lower limb. *J Physiol* 491(Pt 1), 197–207.

Kavounoudias A, Roll R, Roll JP (1999). Specific whole-body shifts induced by frequency-modulated vibrations of human plantar soles. *Neurosci Lett*. 266, 181–184.

Kavounoudias A, Roll R, Roll JP. The plantar sole is a 'dynamometric map' for human balance control (1998). *Neuroreport*. 9, 3247–3252.

Knikou M (2010). Plantar cutaneous afferents normalize the reflex modulation patterns during stepping in chronic human spinal cord injury. *J Neurophysiol* 103, 1304–1314.

Knikou M (2007). Plantar cutaneous input modulates differently spinal reflexes in subjects with intact and injured spinal cord. *Spinal Cord* 45, 69–77.

Li Y, Lucas-Osma AM, Black S, Fenrich KK, Stephens MJ, Sanelli L, Lin S, Fouad K, Goroassini MA, & Bennett DJ (2017). Presynaptic facilitation of the monosynaptic reflex in humans and rats. *Society for Neuroscience* 679.12/DD4.

Lowrey CR, & Bent LR (2009). Modulation of the soleus H-reflex following galvanic vestibular stimulation and cutaneous stimulation in prone human subjects. *Muscle Nerve* 40, 213–220.

Lucas-Osma AM, Li Y, Lin S, et al. (2018). Extrasynaptic α_5GABA$_A$ receptors on proprioceptive afferents produce a tonic depolarization that modulates sodium channel function in the rat spinal cord. *J Neurophysiol* 120, 2953–2974.

Lundberg A, Malmgren K, & Schomburg ED (1977). Cutaneous facilitation of transmission in reflex pathways from Ib afferents to motoneurones. *J Physiol* 265, 763–780.

Maki BE, Perry SD, Norrie RG, & McIlroy WE (1999). Effect of facilitation of sensation from plantar foot-surface boundaries on postural stabilization in young and older adults. *J Gerontol A Biol Sci Med Sci* 54, M281–7.

Meyer PF, Oddsson LI, & De Luca CJ (2004). The role of plantar cutaneous sensation in unperturbed stance. *Exp Brain Res* 156, 505–512.

Mildren RL, Peters RM, Hill AJ, Blouin JS, Carpenter MG, & Inglis JT (2017). Frequency characteristics of human muscle and cortical responses evoked by noisy Achilles tendon vibration. *J Appl Physiol (1985)* 122, 1134–1144.

Mildren RL, Peters RM, Carpenter MG, Blouin JS, Inglis JT (2019). Soleus single motor units show stronger coherence with Achilles tendon vibration across a broad bandwidth relative to medial gastrocnemius units while standing. *J Neurophysiol* 122, 2119–2129.

Morita H, Crone C, Christenhuis D, Petersen NT, & Nielsen JB (2001). Modulation of presynaptic inhibition and disynaptic reciprocal Ia inhibition during voluntary movement in spasticity. *Brain* 124, 826–837.

Morita H, Petersen N, Christensen LO, Sinkjaer T, & Nielsen J (1998). Sensitivity of H-reflexes and stretch reflexes to presynaptic inhibition in humans. *J Neurophysiol* 80, 610–620.

Mynark RG, Koceja DM. (2002). Down training of the elderly soleus H reflex with the use of a spinally induced balance perturbation. *J Appl Physiol (1985)* 93, 127–133.

Nakajima T, Sakamoto M, Tazoe T, Endoh T, Komiyama T (2006). Location specificity of plantar cutaneous reflexes involving lower limb muscles in humans. *Exp Brain Res* 175, 514–525.

Pierrot-Deseilligny E, Bergego C, Katz R, & Morin C (1981). Cutaneous depression of Ib reflex pathways to motoneurones in man. *Exp Brain Res* 42, 351–361.

Pierrot-Deseilligny E, & Burke D (2012). The Circuitry of the Human Spinal Cord: Spinal and Corticospinal Mechanisms of Movement. Cambridge University Press: New York. ISBN: 978-0521192583.

Rossi A, & Mazzocchio R (1988). Cutaneous control of group I pathways from ankle flexors to extensors in man. *Exp Brain Res* 73, 8–14.

Rudomin P, & Schmidt RF (1999). Presynaptic inhibition in the vertebrate spinal cord revisited. *Exp Brain Res* 129, 1–37.

Sayenko DG, Vette AH, Kamibayashi K, Nakajima T, Akai M, & Nakazawa K (2007). Facilitation of the soleus stretch reflex induced by electrical excitation of plantar cutaneous afferents located around the heel. *Neurosci Lett* 415, 294–298.

Sayenko DG, Vette AH, Obata H, Alekhina MI, Akai M, & Nakazawa K (2009). Differential effects of plantar cutaneous afferent excitation on soleus stretch and H-reflex. *Muscle Nerve* 39, 761–769.

van Wezel BM, Ottenhoff FA, & Duysens J (1997). Dynamic control of location-specific information in tactile cutaneous reflexes from the foot during human walking. *J Neurosci* 17, 3804–3814.

van Wezel BM, van Engelen BG, Gabreels FJ, Gabreels-Festen AA, & Duysens J (2000).

Abeta fibers mediate cutaneous reflexes during human walking. *J Neurophysiol* 83, 2980–2986.

Wang Y, Watanabe K, & Chen L (2016). Effect of plantar cutaneous inputs on center of pressure during quiet stance in older adults. *J Exerc Sci Fit* 14, 24–28.

Willis WD (2006). John Eccles' studies of spinal cord presynaptic inhibition. *Prog Neurobiol* 78, 189–214.

Zhan Y, Halliday D, Jiang P, Liu X, & Feng J (2006). Detecting time-dependent coherence between non-stationary electrophysiological signals – a combined statistical and time-frequency approach. *J Neurosci Methods* 156, 322–332.

Zehr EP, Komiyama T, & Stein RB (1997). Cutaneous reflexes during human gait: electromyographic and kinematic responses to electrical stimulation. *J Neurophysiol* 77, 3311–3325.

Zehr EP, & Loadman PM (2012). Persistence of locomotor-related interlimb reflex networks during walking after stroke. *Clin Neurophysiol* 123, 796–807.

Zehr EP, Nakajima T, Barss T, et al. (2014). Cutaneous stimulation of discrete regions of the sole during locomotion produces "sensory steering" of the foot. *BMC Sports Sci Med Rehabil* 6, 33-1847-6-33. eCollection 2014.
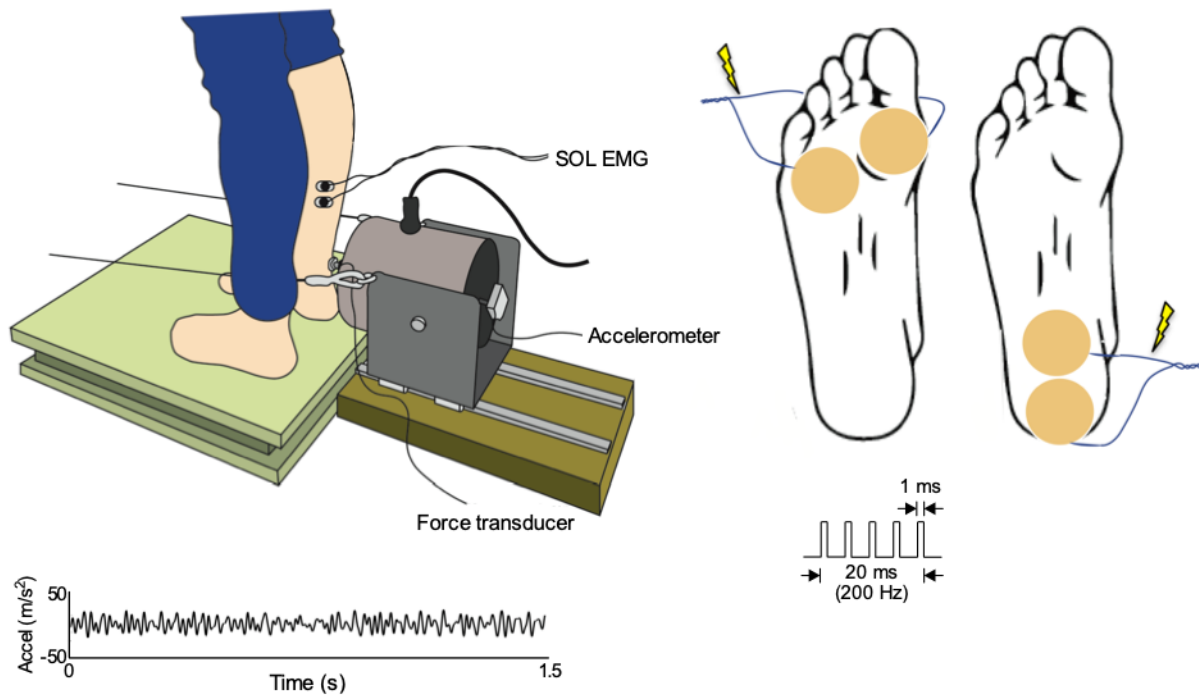
Figure 1. Illustration of the experimental setup.

Illustration of the experimental setup used to apply noisy Achilles tendon vibration along with electrical pulse trains to the heel or metatarsals of the foot sole during standing. A sample of the vibration acceleration profile, as well as the parameters of the cutaneous stimuli, are also demonstrated.
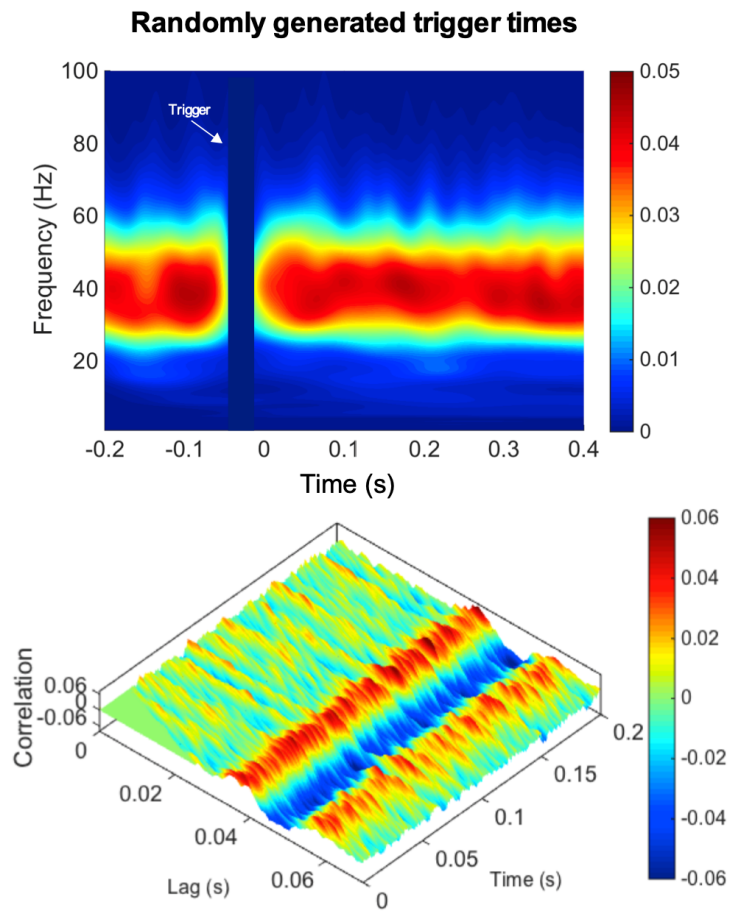
Figure 2. Coherence and cross-correlations over time without the influence of cutaneous stimuli.

Time-dependent coherence and cross-correlations aligned to randomly generated trigger times (i.e., not aligned to electrical stimuli) (n = 12). These data illustrate vibration responses over time that would be expected without cutaneous stimuli. Note there was minimal variation in coherence strength and cross-correlation amplitude over time.
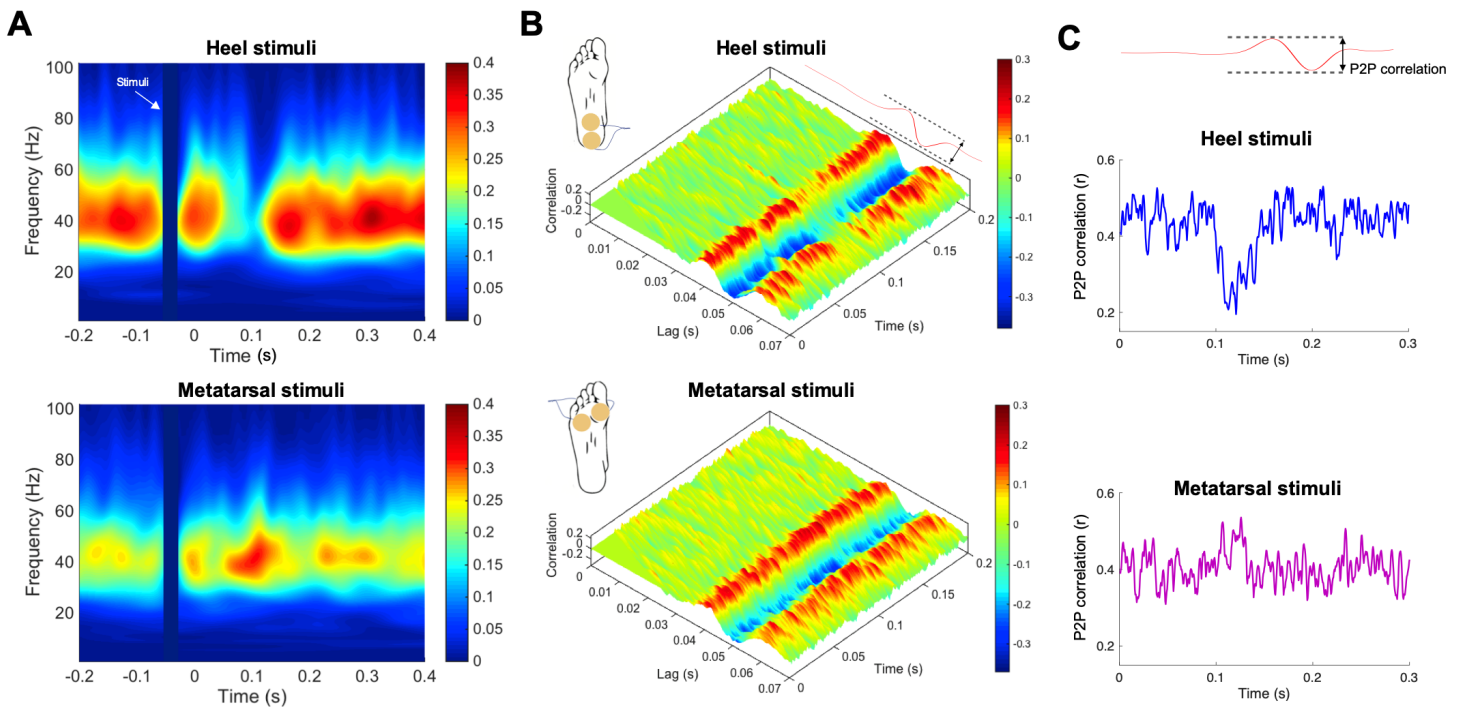
Figure 3. Representative coherence and cross-correlations following heel and metatarsal cutaneous stimuli.

Representative data from one participant of time-dependent vibration-EMG coherence (A) and cross-correlations (B) following cutaneous pulse trains applied to the heel (top panel) and metatarsals (bottom panel). Time (s) is time following the cutaneous pulses, and lag (s) is the cross-correlation lag time. For time-dependent coherence warmer colours reflect stronger coherence, and for time-dependent cross-correlations warmer colours reflect stronger positive correlations and cooler colours reflect stronger negative correlations. The peak-to-peak (P2P) amplitude of the cross-correlations was extracted over time following the cutaneous stimuli and plotted in panel C. Note the suppression in coherence and cross-correlations following heel stimuli and the enhancement following metatarsal stimuli.
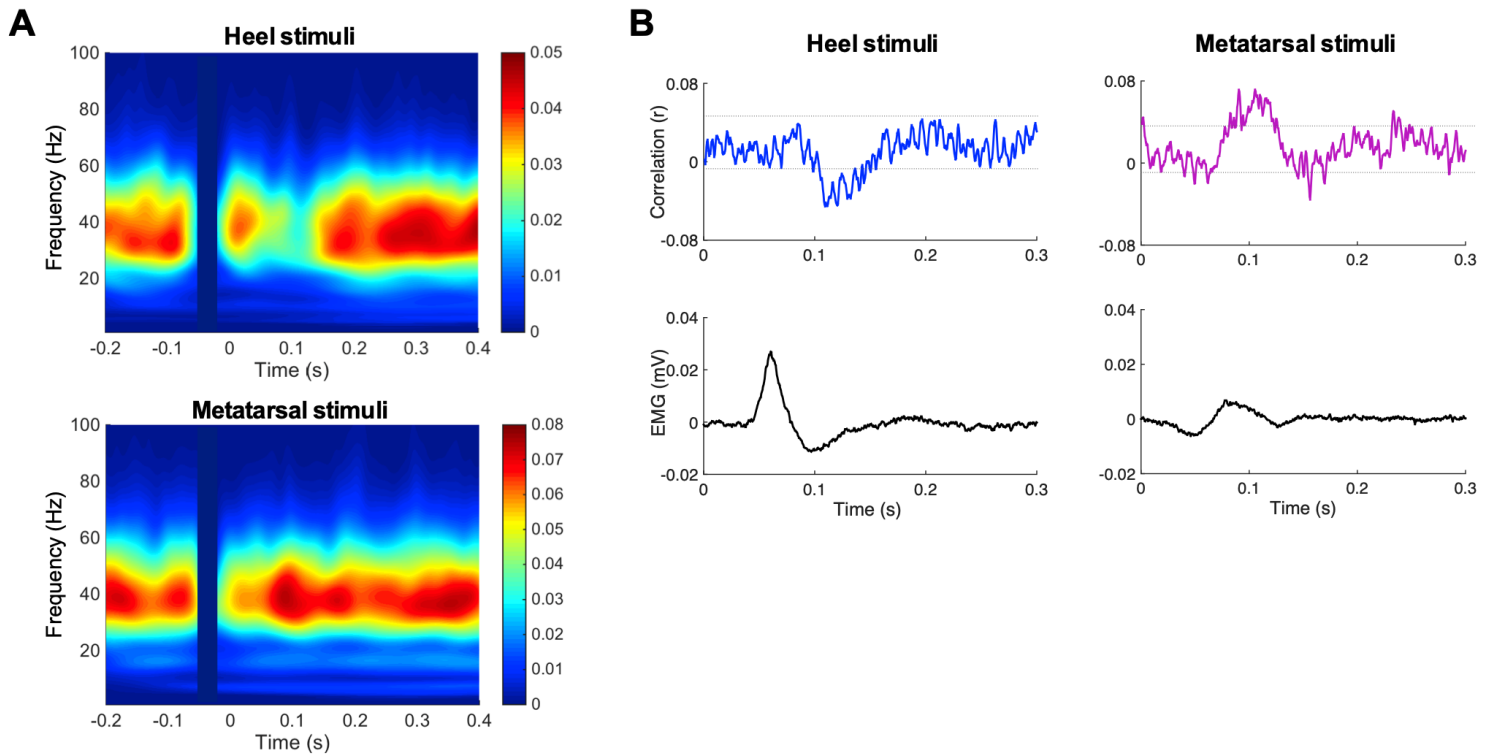
Figure 4. Coherence and changes in cross-correlation amplitude and EMG following heel and metatarsal cutaneous stimuli.

Group results for time-dependent coherence following heel and metatarsal stimuli (n = 12) (A) and the average change in peak-to-peak (P2P) cross correlations following cutaneous stimuli (B; top panel) and the cutaneous reflex in soleus surface EMG (B; bottom panel) (n = 12). Horizontal dotted lines represent 2 SD limits. Note the depression and enhancement in coherence and cross-correlations following heel and metatarsal stimuli, respectively.
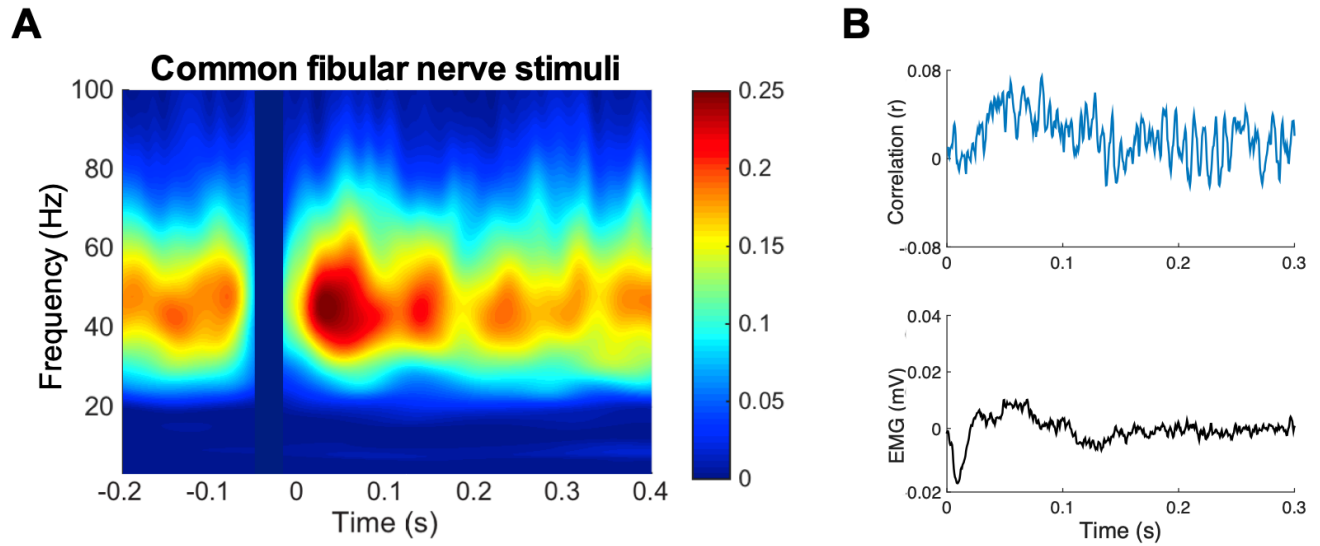
Figure 5. Coherence and changes in cross-correlation amplitude and EMG following common fibular nerve stimuli.

Time-dependent vibration-EMG coherence following common fibular (CF) nerve stimuli (A) and the average change in peak-to-peak cross-correlations and soleus surface EMG following CF nerve stimuli (n = 6) (B). Note the early enhancement in coherence (peak at ~30 ms) and cross-correlations following CF nerve stimuli.
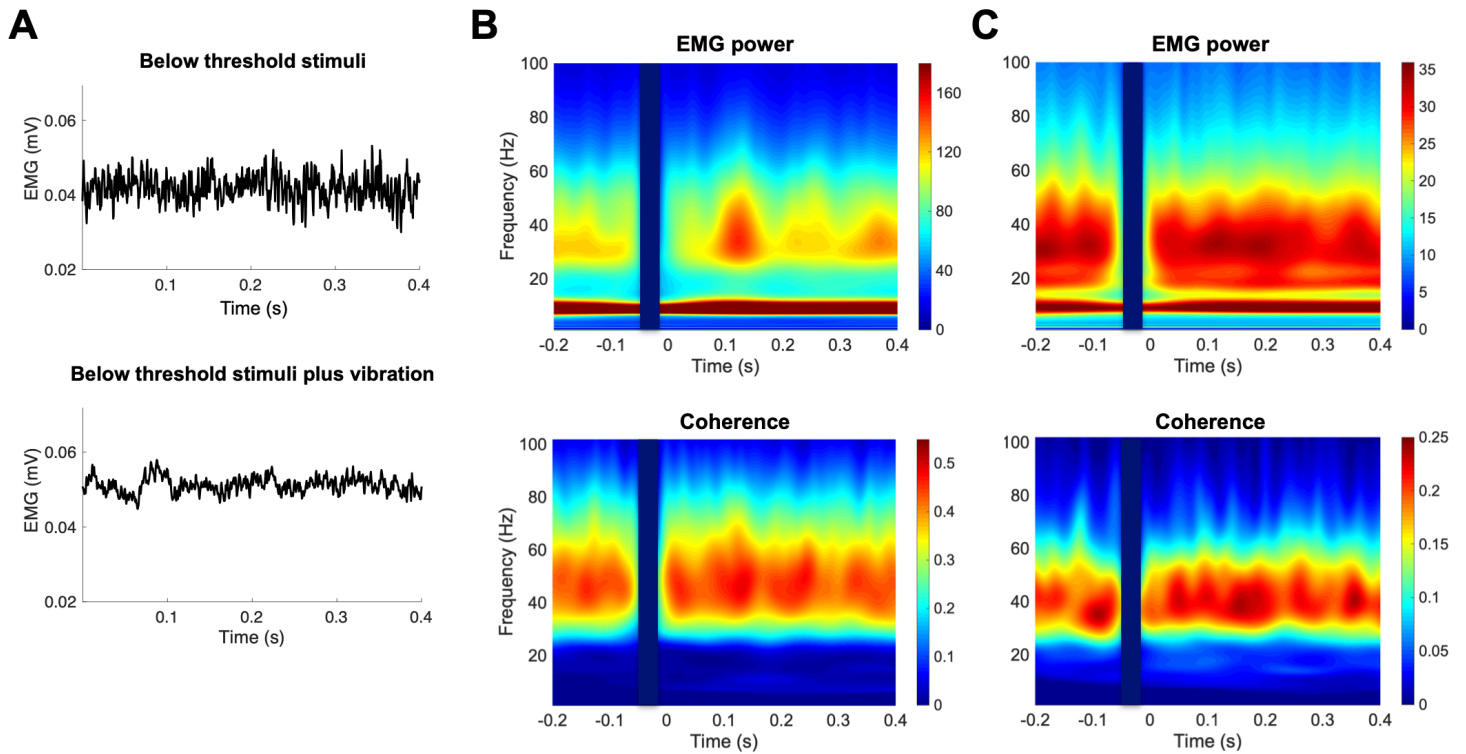
Figure 6. Representative soleus EMG, power, and coherence with lower intensity cutaneous stimuli.

Example of trigger-averaged surface EMG when cutaneous stimuli were delivered below reflex threshold, and trigger-averaged surface EMG at the same stimulus level while vibration was applied (A). Time dependent EMG power and coherence in one participant that demonstrated a cutaneous reflex (increase in EMG power at ~100 ms latency) when vibration was added to previously sub-threshold cutaneous stimuli (B). Data from one participant that did not demonstrate a cutaneous reflex or modulation in vibration-EMG coherence (C). Note that stimuli below the threshold to evoke a change in α-motoneuron pool excitability (i.e., a cutaneous reflex), but likely above the threshold to activate γ-motoneurons, did not evoke a change in time-dependent coherence.